Circuits Syst Signal Process (2011) 30: 527–542
DOI 10.1007/s00034-010-9242-0

New Adaptive All-pass Based Notch Filter for Narrowband/FM Anti-jamming GPS Receivers

Wei-Lung Mao · Wann-Jiun Ma · Ying-Ren Chien · Chia-Hao Ku

Received: 18 May 2009 / Revised: 10 February 2010 / Published online: 29 January 2011

Abstract The global positioning system (GPS), which provides accurate positioning and timing information, has become a commonly used navigation instrument for many applications. The application of a new adaptive all-pass based notch filter (ANFA) for narrowband/FM interference suppression and frequency estimation in GPS receivers is proposed. An ANFA structure that achieves better unbiased characteristics with its coefficients is employed to accurately estimate the narrowband interfering signals in online fashion. A variable convergence factor that optimizes the maximal mean square error (MSE) reduction in each iteration is applied in a modified adaptive Gaussian–Newton (MAGN) algorithm. The proposed MAGN algorithm can lead to both faster convergence speed and higher estimation accuracy. Simulation results show that the ANFA offers a better performance than conventional linear predictors in terms of the SNR improvement and the mean output power (MOP) under the interference environments of interest.

W.-L. Mao (✉)
Department of Electronic Engineering, National Formosa University, No. 64, Wunhua Road, Huwei Township, 63210 Yunlin County, Taiwan, ROC
e-mail: wlmao123@yahoo.com.tw

W.-L. Mao (✉)
e-mail: wlmao@nfu.edu.tw

W.-J. Ma
Department of Electrical Engineering, National Taiwan University, Taipei 10617, Taiwan, ROC
e-mail: r91921118@ntu.edu.tw

Y.-R. Chien
Integrated Logistical Support Center, Chung-Shan Institute of Science and Technology, Taoyuan, Taiwan, ROC
e-mail: curtis@citi.sinica.edu.tw

C.-H. Ku
Department of Electrical Engineering, Mingchi University of Technology, Taipei, Taiwan, ROC
e-mail: kuchiahao@mail.mcut.edu.tw

Birkhäuser

Keywords Global Positioning System (GPS) · Modified adaptive Gauss–Newton (MAGN) algorithm · Adaptive All-pass based Notch Filter (ANFA) · Interference Suppression

1 Introduction

A GPS receiver can provide accurate positioning and timing information by processing its received navigation data. Usually, GPS spread spectrum signals are 20–30 dB below background thermal noise. Depending on its signal characteristics, GPS inherently has a certain degree of protection against intentional and unintentional interfering signals due to the despreading gain. However, if jamming strength is higher than the system's processing gain, GPS performance can be degraded severely. Therefore, it is necessary to develop additional techniques for protection of the GPS in jamming environments.

There are several approaches to mitigating the narrowband interference, including time domain techniques [8], frequency domain techniques [3], and time-frequency domain techniques [4, 7]. Recently, time-frequency distribution (TFD) methods [1, 2, 9] have been developed to effectively estimate the instantaneous frequency of parametric signals imbedded in noise. Once the parameters have been extracted, an adaptive time-varying filter can be established to reject the obstacle. The estimation of instantaneous frequency plays an important role in this FM suppression technique. However, errors in instantaneous frequency may occur in many conditions due to a decline in interference power, the presence of AM [2], or high levels of cross-terms in the TF domain.

It has been shown that the adaptive notch filter (ANF) [5–7] is a superior filtering approach to decomposing a received signal into the narrowband and broadband components, and thereby the narrowband part can be eliminated successfully. The IIR-based adaptive filters have better statistical performances than adaptive FIR, with fewer coefficients and lower computational costs. The minimal parameter constrained notch filter (CNF) [6] is proposed for elimination of multiple unknown sine waves imbedded in a broadband signal. However, the coefficients biased problem is still a challenge that needs to be overcome in CNF design. It has also been proved [10] that the adaptive all-pass based notch filter (ANFA) has a better unbiased property with its coefficients, both theoretically and experimentally. Through the various consumer and aerospace GPS applications, the adequate ANFA structure can be employed to converge instantaneously to the incident frequency and track the variation of interfering signals.

This study investigates the applicability of ANFA for interference suppression and frequency estimation in GPS receivers. Since the characteristics of interference are always unknown or time-variant, the notch point of ANFA can be adjusted adaptively to cancel the narrowband component from its input waveforms. The variable convergence factor that minimizes the instantaneous error criterion is adopted in the modified adaptive Gaussian–Newton (MAGN) algorithm to enhance the convergence speed. Four kinds of interfering signals are considered. They are: (1) single-tone continuous wave interference (CWI), (2) multi-tone CWI, (3) pulsed CWI, and (4) linear

FM signals. The improved performances of the ANFA scheme are compared with that of the conventional normalized least mean square (NLMS) and recursive least squares (RLS) in terms of the SNR improvement and mean output power (MOP) under the diversity of stationary and time-varying jamming environments.

2 Received Signal Models

A simplified block diagram of the anti-jamming GPS model is shown in Fig. 1(a). The transmitted spread spectrum signal is given by:

$$Z(t) = \big[B(t) \oplus CA(t)\big]\cos(\omega_{L1}t) \tag{1}$$

where $B(t)$ represents the transmitted baseband navigation data which is in binary form and has a duration T ($T = 20$ ms). $CA(t)$ is the GPS course acquisition (C/A) code sequence with chip duration T_c ($R_c = 1/T_c = 1.023$ MHz), and $L1$ represents primary GPS frequency (1575.42 MHz). The integer $PG = T/T_c = 20460 = 43$ (dB) is the processing gain of the GPS system.

The jamming signals may be intentional or unintentional. Intentional signals are always hostile. Friendly sources originate from RF transmitters, which are either nearby ground RF transmission stations or those on-board aircraft. Four kinds of jamming signals are investigated:

(1) Single-tone CWI:

$$J_{\text{scwi}}(t) = A\cos\big[(\omega_{L1} + \omega_{\Delta})t + \theta\big] \tag{2a}$$

where A denotes the amplitude and ω_{Δ} is its frequency offset from the central frequency of the spread spectrum signal. θ is a random phase uniformly distributed over the interval $[0, 2\pi)$.

(2) Multi-tone CWI:

$$J_{mcwi}(t) = \sum_{i=1}^{m} A_i \cos\big[(\omega_{L1} + \omega_{\Delta i})t + \theta_i\big] \tag{2b}$$

where m, A_i, $\omega_{\Delta i}$, and θ_i represent the numbers of narrowband jamming, amplitude, frequency offset, and random phase of the ith interference, respectively.

(3) Pulsed CWI:

$$J_{\text{pcwi}}(t) = \begin{cases} A\cos\big[(\omega_{L1} + \omega_{\Delta})t + \theta\big] & (l-1)N_T \le t < (l-1)N_T + N_1, \\ 0 & (l-1)N_T + N_1 \le t < lN_T, \end{cases} \tag{2c}$$

where the on-interval is $N_1 T_c$ seconds long and the off-interval is $(N_T - N_1)T_c$ seconds long. The case in which N_T and N_1 are much greater than unity is considered.

(4) Linear FM (swept CWI):

$$J_{\text{swcwi}}(t) = A\cos\big[0.5 * \alpha_{\Delta} t^2 + (\omega_{L1} + \omega_{\Delta})t + \theta\big] \tag{2d}$$

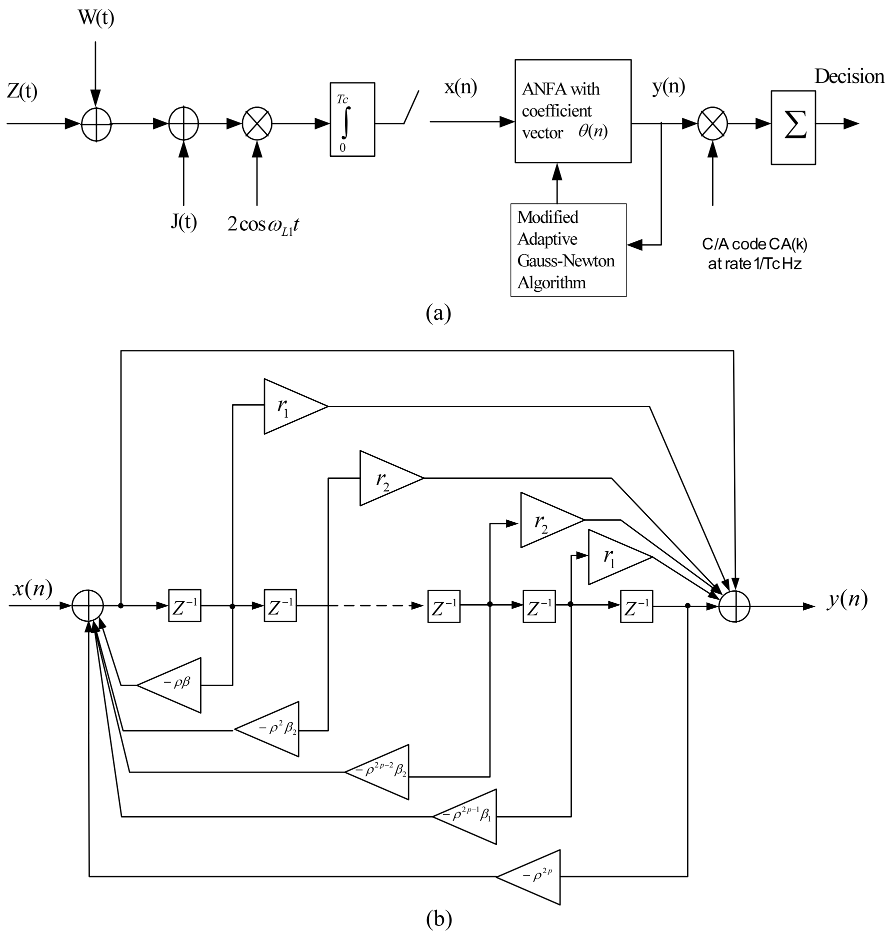

Fig. 1 (**a**) Block diagram of the GPS anti-jamming system and (**b**) Architecture of the all-pass based notch filter

where A is the amplitude of signal, and α_Δ and ω_Δ represent its frequency rate and offset frequency, respectively.

The received signal is band-pass filtered, amplified, and down-converted. To further simplify the analysis, the received signal is sampled at the chip rate. The received observation is

$$x(n) = Z(n) + J(n) + W(n) \tag{3}$$

where $W(n)$ is additive white Gaussian noise (AWGN) with variance σ^2, and the jamming source $J(n)$ of interest has a bandwidth much narrower than $1/T_c$. These three components are assumed to be mutually independent.

Figure 1(a) shows the block diagram of the GPS anti-jamming system. The proposed adaptive NFA is used to suppress a variety of jamming signals. This method exploits the property that the GPS spread spectrum signals are difficult to track, whereas a large class of interferences, such as narrowband and FM signals, can be blocked from the NFA notch frequency. The adaptive NFA filter is utilized to reject narrowband/FM interference in the GPS system. Following the filtering from the received waveform, the output of canceller, $y(n)$, can be written as

$$y(n) = T(n) * x(n) = T(n) * \{Z(n) + J(n) + W(n)\} \cong Z(n) + W(n) \tag{4}$$

where $T(n)$ is the impulse response of the NFA, $*$ denotes the convolution operation, and $y(n)$ is the broadband component of the received signal. It can be viewed as an almost interference-free signal and is fed into the correlator for further despreading.

3 All-Pass Based Notch Filter (NFA)

3.1 Second-Order IIR Filter Parameterization

First, the second-order all-pass based notch filter (NFA) [10] of interest can be written as

$$T_1(z) = \frac{1}{2}\big[1 + A_1(z)\big] = \frac{1}{2}\left[1 + \frac{a_2 - a_1 z^{-1} + z^{-2}}{1 - a_1 z^{-1} + a_2 z^{-2}}\right] \tag{5a}$$

with $a_1 = \frac{2\cos\omega_z}{1+\tan(BW/2)}$, and $a_2 = \frac{1-\tan(BW/2)}{1+\tan(BW/2)} = \rho^2$ where $A_1(z)$ is a second-order all-pass function, ω_z is the angle of zero of $T_1(z)$, BW represents the -3 dB notch bandwidth of zero of $T_1(z)$, and ρ is the pole radius of zero of $T_1(z)$. Because of the symmetry, only the upper side of the z-plane is discussed, i.e. $\omega_z \in [0, \pi]$. The parameter ρ should be less than unity for stability. Inserting the pole $z = \rho e^{jw_p}$ (ω_p is the pole angle) into (5a), the pole/zero angles can be obtained as

$$\cos\omega_z = \frac{a_1}{1 + a_2} \quad \text{and} \quad \cos\omega_p = \frac{a_1}{2\sqrt{a_2}} = \frac{a_1}{2\rho}. \tag{5b}$$

3.2 $2p$th-Order IIR Filter Parameterization

A $2p$th-order all-pass based notch filter trained with the MAGN algorithm is proposed in our work. The general transfer function of $2p$th-order NFA is represented as

$$\begin{aligned} T(z) &= \frac{1}{2}\big[1 + A(z)\big] = \frac{1}{2}\left[1 + \frac{\prod_{i=1}^{p}(\rho^2 - 2\cos(\omega_{p,i})\rho z^{-1} + z^{-2})}{\prod_{i=1}^{p}(1 - 2\cos(\omega_{p,i})\rho z^{-1} + \rho^2 z^{-2})}\right] \\ &= \frac{\prod_{i=1}^{p}(\rho^2 + \rho\beta_i z^{-1} + z^{-2}) + \prod_{i=1}^{p}(1 + \rho\beta_i z^{-1} + \rho^2 z^{-2})}{2[\prod_{i=1}^{p}(1 + \rho\beta_i z^{-1} + \rho^2 z^{-2})]} \end{aligned} \tag{6}$$

with $\beta_i = -2\cos(\omega_{p,i})$ where p is the total number of notch frequencies, $A(z)$ is a $2p$th-order all-pass function, and $\omega_{p,i}$ is the ith pole angle. In order to obtain the formulation of the filter coefficients and characteristics in the CNF form, the relations between both CNF and the NFA must be analyzed and compared. The following general constrained form of the $2p$th-order notch filter [6] is represented as:

$$T_{\mathrm{CNF}}(z)=\frac{\prod_{i=1}^{p}(1-2\cos(\omega_i)z^{-1}+z^{-2})}{\prod_{i=1}^{p}(1-2\cos(\omega_i)\rho z^{-1}+\rho^2z^{-2})}=\frac{\prod_{i=1}^{p}(1+r_iz^{-1}+z^{-2})}{\prod_{i=1}^{p}(1+\rho r_iz^{-1}+\rho^2z^{-2})} \tag{7}$$

with $r_i=-2\cos(\omega_i)$ where ω_i is the ith notch frequency. Let $T(z)$ and $T_{\mathrm{CNF}}(z)$ have the same numerator and denominator polynomials. Then, the transfer function $T(z)$ of NFA and the corresponding coefficients can be derived and formulated as

$$\begin{aligned}T(z)&=\frac{N(z^{-1})}{N(\rho z^{-1})}\\&=\frac{1+r_1z^{-1}+\cdots+r_pz^{-p}+\cdots+r_1z^{-2p+1}+z^{-2p}}{1+\rho\beta_1z^{-1}+\cdots+\rho^p\beta_pz^{-p}+\cdots+\rho^{2p-1}\beta_1z^{-2p+1}+\rho^{2p}z^{-2p}}\\&=\frac{1+r_1z^{-1}+\cdots+r_pz^{-p}+\cdots+r_1z^{-2p+1}+z^{-2p}}{1+\rho\frac{1+\rho^{2p}}{\rho^1+\rho^{2p-1}}r_iz^{-1}+\cdots+\rho^p\frac{1+\rho^{2p}}{2\rho^p}r_iz^{-p}+\cdots+\rho^{2p-1}\frac{1+\rho^{2p}}{\rho^1+\rho^{2p-1}}z^{-2p+1}+\rho^{2p}z^{-2p}}\end{aligned} \tag{8}$$

with $\beta_i=\frac{1+\rho^{2p}}{\rho^i+\rho^{2p-i}}r_i$, $i=1,\ldots p$.

Figure 1(b) shows in detail the realization structure of the proposed all-pass based notch filter. This adaptive notch filter is utilized to estimate the sinusoidal frequencies and consequently eliminates the corresponding sinusoidal waveforms at its notch frequencies.

4 Modified Adaptive Gauss–Newton (MAGN) Algorithm

The MAGN algorithm is designed to estimate the filter parameters of the NFA structure, and some additional modifications are applied to increase the convergence speed [5]. The input–output relation of a notch filter can be represented in a difference equation [9]:

$$y(n)=x(n)+x(n-2p)-\rho^{2p}(n)y(n-2p)-\varphi^T(n)\theta(n-1) \tag{9}$$

with $\varphi(n)=\begin{bmatrix}\varphi_1(n) & \varphi_2(n) & \cdots & \varphi_p(n)\end{bmatrix}^T$

$$\varphi_i(n)=\begin{cases}-x(n-i)-x(n-2p+i)+[\rho^i(n)y(n-i)+\rho^{2p-i}(n)y(n-2p+i)]\\ \quad\times\frac{1+\rho^{2p}(n)}{\rho^i(n)+\rho^{2p-i}(n)} & 1\le i\le(p-1)\\ -x(n-i)+\rho^p(n)y(n-p)\frac{1+\rho^{2p}(n)}{2\rho^{2p}(n)} & i=p\end{cases}$$

where p is the total number of notches, $\rho(n)$ is a positive real number close to but smaller than 1, $x(n)$ is the input signal, and $y(n)$ is the broadband output signal. The filter parameter vector $\theta(n)$ is defined as

$$\theta(n)=\begin{bmatrix}r_1(n) & r_2(n) & \cdots & r_p(n)\end{bmatrix}^T \tag{10}$$

where the $r_j(n)$ are the filter coefficients. The vector $\theta(n)$ will be adjusted by minimizing the notch filter output power $E|y(n)|^2$. The negative gradient vector $\mathbf{\Psi}(n)$ [6] is defined as:

$$\begin{aligned}\mathbf{\Psi}(n) &= -\nabla[y(n)] = \begin{bmatrix}\Psi_1(n) & \Psi_2(n) & \cdots & \Psi_p(n)\end{bmatrix} \\ &= \begin{bmatrix}-\dfrac{\partial y(n)}{\partial r_1(n)} & -\dfrac{\partial y(n)}{\partial r_2(n)} & \cdots & -\dfrac{\partial y(n)}{\partial r_p(n)}\end{bmatrix}\end{aligned} \tag{11}$$

with

$$\Psi_i(n) = \begin{cases} -x(n-i) - x(n-2p+i) + [\rho^i(n)y(n-i) + \rho^{2p-i}(n)y(n-2p+i)] \\ \quad \times \frac{1+\rho^{2p}(n)}{\rho^i(n)+\rho^{2p-i}(n)} \quad 1 \le i \le (p-1) \\ -x(n-i) + \rho^p(n)y(n-p)\frac{1+\rho^{2p}(n)}{2\rho^{2p}(n)} \quad i = p. \end{cases}$$

4.1 MAGN Adaptation Method

According to the derivation results above, the MAGN algorithm can be formulated by the following recursions. This adaptation algorithm for updating the coefficients of IIR filter $\theta(n)$ is based on the MAGN method to increase the rate of convergence and reduce the mean output power.
Initialization: Some initialization variables are selected as follows: $\theta(0) = \begin{bmatrix}0 & 0 & \cdots & 0 & 1\end{bmatrix}^T$, $\boldsymbol{P}(0) = \mu \mathbf{I}_p$ where $\mathbf{I}_p$ is a p-by-p identity matrix, $\psi(0) = 0$, and $x(-i) = 0$ where $i = 1, \dots, 2p$.
Normal Values: $\sigma = 100/E(|x(n)|^2)$, $\lambda_0 = 0.8$, $\lambda(1) = 0.9$, $\rho_0 = 0.84$ and $\rho(1) = 0.8$ and $\rho(\infty) = 0.995$.
Algorithm:
For each $x(n)$ given for $n \ge 0$, compute:

$$\varphi(n) = \begin{bmatrix}\varphi_1(n) & \varphi_2(n) & \cdots & \varphi_p(n)\end{bmatrix}^T \tag{12a}$$

with

$$\varphi_i(n) = \begin{cases} -x(n-i) - x(n-2p+i) + \left[\rho^i(n)\bar{y}(n-i) + \rho^{2p-i}(n)\bar{y}(n-2p+i)\right] \\ \quad \times \frac{1+\rho^{2p}(n)}{\rho^i(n)+\rho^{2p-i}(n)} \quad 1 \le i \le (p-1), \\ -x(n-i) + \rho^p(n)\bar{y}(n-p)\frac{1+\rho^{2p}(n)}{2\rho^{2p}(n)} \quad i = p, \end{cases}$$

$$y(n) = x(n) + x(n-2p) - \rho^{2p}(n)\bar{y}(n-2p) - \varphi^T(n)\widehat{\theta}(n-1) \tag{12b}$$

$$\mathbf{\Psi}(n) = \begin{bmatrix}\Psi_1(n) & \Psi_2(n) & \cdots & \Psi_p(n)\end{bmatrix} \tag{12c}$$

with

$$\Psi_i(n) = \begin{cases} -x_F(n-i) - x_F(n-2p+i) \\ \quad + [\rho^i(n)\bar{y}_F(n-i) + \rho^{2p-i}(n)\bar{y}_F(n-2p+i)]\frac{1+\rho^{2p}(n)}{\rho^i(n)+\rho^{2p-i}(n)} \\ \quad 1 \le i \le (p-1), \\ -x_F(n-i) + \rho^p(n)\bar{y}_F(n-p)\frac{1+\rho^{2p}(n)}{2\rho^{2p}(n)} \quad i = p, \end{cases}$$

$$\alpha(n)=\frac{2}{1+\sqrt{2\Psi^T(n)P(n-1)\Psi(n)-1}} \tag{12d}$$

$$\boldsymbol{P}(n)=\frac{1}{\lambda(n)}\left[\boldsymbol{P}(n-1)-\frac{\boldsymbol{P}(n-1)\boldsymbol{\Psi}(n)\boldsymbol{\Psi}^H(n)\boldsymbol{P}(n-1)}{\lambda(n)/\alpha(n)+\boldsymbol{\Psi}^H(n)\boldsymbol{P}(n-1)\boldsymbol{\Psi}(n)}\right] \tag{12e}$$

$$\widehat{\theta}(n)=\widehat{\theta}(n-1)+\alpha(n)\boldsymbol{P}(n)\boldsymbol{\Psi}(n)y(n). \tag{12f}$$

Check stability and use the stability projection method:

$$\bar{y}(n)=x(n)+x(n-2p)-\rho^{2p}(n)\bar{y}(n-2p)-\varphi^T(n)\widehat{\theta}(n) \tag{12g}$$

$$\begin{aligned}\bar{y}_F(n)&=\bar{y}(n)+\rho^{2p}(n)\bar{y}_F(n-2p)-\rho^P(n)\bar{y}_F(n-p)\hat{r}_p(n)\frac{1+\rho^{2p}(n)}{2\rho^{2p}(n)}\\&\quad-\sum_{i=1}^{p-1}\left[\rho^i(n)y_F(n-i)+\rho^{2p-i}(n)y_F(n-2p+i)\right]\hat{r}_i(n)\frac{1+\rho^{2p}(n)}{\rho^i(n)+\rho^{2p-i}(n)}\end{aligned} \tag{12h}$$

$$\begin{aligned}x_F(n)&=x(n)+\rho^{2p}(n)x_F(n-2p)-\rho^P(n)x_F(n-p)\hat{r}_p(n)\frac{1+\rho^{2p}(n)}{2\rho^{2p}}\\&\quad-\sum_{i=1}^{p-1}\left[\rho^i(n)x_F(n-i)+\rho^{2p-i}(n)x_F(n-2p+i)\right]\hat{r}_i(n)\frac{1+\rho^{2p}(n)}{\rho^i(n)+\rho^{2p-i}(n)}\end{aligned} \tag{12i}$$

$$\lambda(n+1)=\lambda_0\lambda(n)+(1-\lambda_0) \tag{12j}$$

$$\rho(n+1)=\rho_0\rho(n)+(1-\rho_0)\rho(\infty) \tag{12k}$$

where $\lambda(n)$ is the forgetting factor, $\widehat{\theta}(n)=\left[\widehat{r}_1(n) \quad \widehat{r}_2(n) \quad \cdots \quad \widehat{r}_p(n)\right]^T$ is the estimated filter parameter vector, $\boldsymbol{P}(n)$ is the inverse Hessian matrix, i.e., $P(n)=R(n)^{-1}$, $\boldsymbol{R}(n)$ is the Hessian matrix of the performance function $E|y(n)|^2$ with respect to $\hat{\theta}$ evaluated at $\hat{\theta}(n-1)$, and $\alpha(n)$ is the convergence factor [4] which determines the convergence speed of the algorithm. The filtered input and output are given in the form $x_F(n)=x(n)/N(\rho z^{-1},n)$, $y_F(n)=y(n)/N(\rho z^{-1},n)$. Because the ANFA is of the IIR type, a stability checking process in (12g) should be adopted in each iteration. If the distances from the estimated poles to the origin are larger than unity, the poles are replaced with poles of identical angles and reciprocal radii. These updated poles are used to compute the new coefficients of the ANFA for the next adaptation.

4.2 Optimal Convergence Factor

The choice of convergence factor has a considerable effect on the convergence of the MAGN scheme. The variable convergence factor $\alpha(n)$, which optimizes the reduction of MSE in each iteration, is utilized to accomplish faster characteristics. In the neighborhood of a given point of the MSE surface, the variable MSE $\varepsilon(n)$ can be approximated by the quadratic function

$$\varepsilon(n)=\frac{|y(n)|^2}{2}\approx\frac{|x(n)+x(n-2p)-\rho^{2p}(n)\bar{y}(n-2p)|^2}{2}+\hat{\theta}^T(n-1)\eta(n)+\frac{1}{2}\hat{\theta}^T(n-1)\boldsymbol{R}(n-1)\hat{\theta}(n-1) \tag{13}$$

where $\eta(n)$ is defined as. $\nabla_\theta\varepsilon(n)|_{\theta=0}$. Differentiating (13) with respect to $\hat{\theta}$ yields an expression for $\eta(n)$:

$$\eta(n)=\nabla\varepsilon(n)-\boldsymbol{R}(n-1)\hat{\theta}(n-1). \tag{14}$$

In the process of iteration, $\varepsilon(k)$can be replaced by its a posteriori estimate

$$\begin{aligned}\hat{\varepsilon}(n)&=\frac{|\bar{y}(n)|^2}{2}\\&\approx\frac{|x(n)+x(n-2p)-\rho^{2p}(n)\bar{y}(n-2p)|^2}{2}+\big[\hat{\theta}(n-1)+\Delta\theta(n)\big]^T\eta(n)\\&\quad+\frac{1}{2}\big[\hat{\theta}(n-1)+\Delta\theta(n)\big]^T\boldsymbol{R}(n-1)\big[\hat{\theta}(n-1)+\Delta\theta(n)\big]\\&=\varepsilon(n)+\Delta\theta(n)^T\eta(n)+\frac{1}{2}\Delta\theta(n)^T\boldsymbol{R}(n-1)\hat{\theta}(n-1)\\&\quad+\frac{1}{2}\hat{\theta}(n-1)^T\boldsymbol{R}(n-1)\Delta\theta(n)+\frac{1}{2}\Delta\theta(n)^T\boldsymbol{R}(n-1)\Delta\theta(n).\end{aligned} \tag{15}$$

By inserting (14) into (15), it can be shown that

$$\begin{aligned}\Delta\varepsilon(n)&=\hat{\varepsilon}(n)-\varepsilon(n)\\&=\Delta\theta(n)^T\big[\nabla\varepsilon(n)-\boldsymbol{R}(n-1)\hat{\theta}(n-1)\big]+\frac{1}{2}\Delta\theta(n)^T\boldsymbol{R}(n-1)\hat{\theta}(n-1)\\&\quad+\frac{1}{2}\hat{\theta}(n-1)^T\boldsymbol{R}(n-1)\Delta\theta(n)+\frac{1}{2}\Delta\theta(n)^T\boldsymbol{R}(n-1)\Delta\theta(n)\\&=\Delta\theta(n)^T\nabla\varepsilon(n)+\frac{1}{2}\Delta\theta(n)^T\boldsymbol{R}(n-1)\Delta\theta(n).\end{aligned} \tag{16}$$

For the Gauss–Newton method, the variable $\Delta\theta(n)$ is represented as:

$$\Delta\theta(n)=\hat{\theta}(n)-\hat{\theta}(n-1)=-\alpha(n)\boldsymbol{R}^{-1}(n)\nabla\varepsilon(n)=-\alpha(n)\boldsymbol{P}(n)\nabla\varepsilon(n) \tag{17}$$

with $\nabla\varepsilon(n)=\nabla[\frac{|y(n)|^2}{2}]=y(n)\nabla y(n)=-y(n)\boldsymbol{\Psi}(n)$.

By inserting (17) into (16), the equation becomes

$$\begin{aligned}\Delta\varepsilon(n) &= -\alpha(n)\nabla\varepsilon^T(n)\boldsymbol{R}^{-T}(n)\nabla\varepsilon(n) + \frac{1}{2}\alpha^2(n)\nabla\varepsilon^T(n)\boldsymbol{R}^{-T}(n)\nabla\varepsilon(n) \\ &= \left[\frac{1}{2}\alpha^2(n) - \alpha(n)\right]\nabla\varepsilon^T(n)\boldsymbol{P}(n)\nabla\varepsilon(n).\end{aligned} \tag{18}$$

By employing the expression $\boldsymbol{P}(n+1)$ in [4], we get

$$\begin{aligned}\Delta\varepsilon(n) &= \left[\frac{1}{2}\alpha^2(n) - \alpha(n)\right]\left|y(n)\right|^2\boldsymbol{\Psi}^T(n)\boldsymbol{P}(n)\boldsymbol{\Psi}(n) \\ &= -\left|y(n)\right|^2\frac{(1-\frac{\alpha(n)}{2})}{(1-\alpha(n))}\left\{\alpha(n)\boldsymbol{\Psi}^T(n)\boldsymbol{P}(n)\boldsymbol{\Psi}(n)\right. \\ &\quad \left. - \frac{\alpha^2(n)[\boldsymbol{\Psi}^T(n)\boldsymbol{P}(n)\boldsymbol{\Psi}(n)]^2}{1-\alpha(n)+\alpha(n)\boldsymbol{\Psi}^T(n)\boldsymbol{P}(n)\boldsymbol{\Psi}(n)}\right\} \\ &= \left|y(n)\right|^2\boldsymbol{\Psi}^T(n)\boldsymbol{P}(n-1)\boldsymbol{\Psi}(n)\frac{\frac{1}{2}\alpha^2(n)-\alpha(n)}{1+\alpha(n)[\boldsymbol{\Psi}^T(n)\boldsymbol{P}(n-1)\boldsymbol{\Psi}(n)-1]}.\end{aligned} \tag{19}$$

From (19), the optimal factor $\alpha(n)$ that leads to maximal mean square error (MSE) reduction is obtained by setting the corresponding derivative to zero. It is found by letting

$$\frac{\partial\Delta\varepsilon(n)}{\partial\alpha(n)} = 0, \tag{20}$$

the equation becomes

$$\alpha^2(n)\big[\boldsymbol{\Psi}^T(n)\boldsymbol{P}(n-1)\boldsymbol{\Psi}(n)-1\big] + 2\alpha(n) - 2 = 0 \tag{21}$$

with

$$\alpha(n) = \frac{-1+\sqrt{2\boldsymbol{\Psi}^T(n)\boldsymbol{P}(n-1)\boldsymbol{\Psi}(n)-1}}{[\boldsymbol{\Psi}^T(n)\boldsymbol{P}(n-1)\boldsymbol{\Psi}(n)-1]} = \frac{2}{1+\sqrt{2\boldsymbol{\Psi}^T(n)\boldsymbol{P}(n-1)\boldsymbol{\Psi}(n)-1}}.$$

The optimal step size can be obtained as [5]:

$$\alpha_{\text{optimal}}(n) = \frac{2}{1+\sqrt{2\boldsymbol{\Psi}^T(n)\boldsymbol{P}(n-1)\boldsymbol{\Psi}(n)-1}} \tag{22}$$

after some manipulation, where $\alpha_{\text{optimal}}(n)$ is the optimal convergence factor. It can be applied in (12d) as the MAGN adaptation algorithm is executed. If $[2\boldsymbol{\Psi}^T(n)\boldsymbol{P}(n-1)\boldsymbol{\Psi}(n)-1]$ is less than zero, it should be replaced by zero in each iteration.

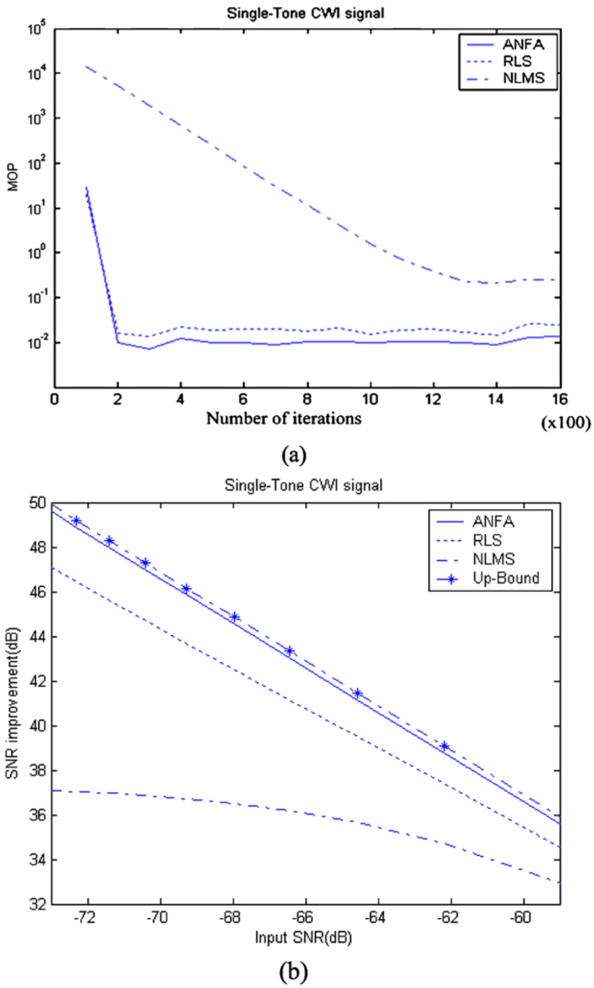

Fig. 2 (**a**) Average MOP $Y_{\mathrm{MOP}}(k)$ vs. the number of iterations and (**b**) SNR improvement for single-tone interference suppression

5 Simulation Results

The simulation results of the MAGN-based ANFA were obtained to confirm the jamming rejection and frequency estimation characteristics. Two indexes were used to verify the performances in transient and steady states in terms of mean output power (MOP) and SNR improvement [8], respectively. They are defined as:

$$Y_{\mathrm{MOP}}(k) = \left\{ \frac{1}{100} \left[\sum_{n=(k-1)*100+1}^{k*100} y^2(n) \right] \right\}, \tag{23a}$$

$$SNR_{\mathrm{improvement}} = 10 \log \left\{ \frac{E[x(n) - Z(n)]^2}{E[y(n) - Z(n)]^2} \right\} \text{ (dB)}, \tag{23b}$$

Fig. 3 (**a**) Average MOP $Y_{\mathrm{MOP}}(k)$ vs. the number of iterations and (**b**) SNR improvement for multi-tone interference suppression

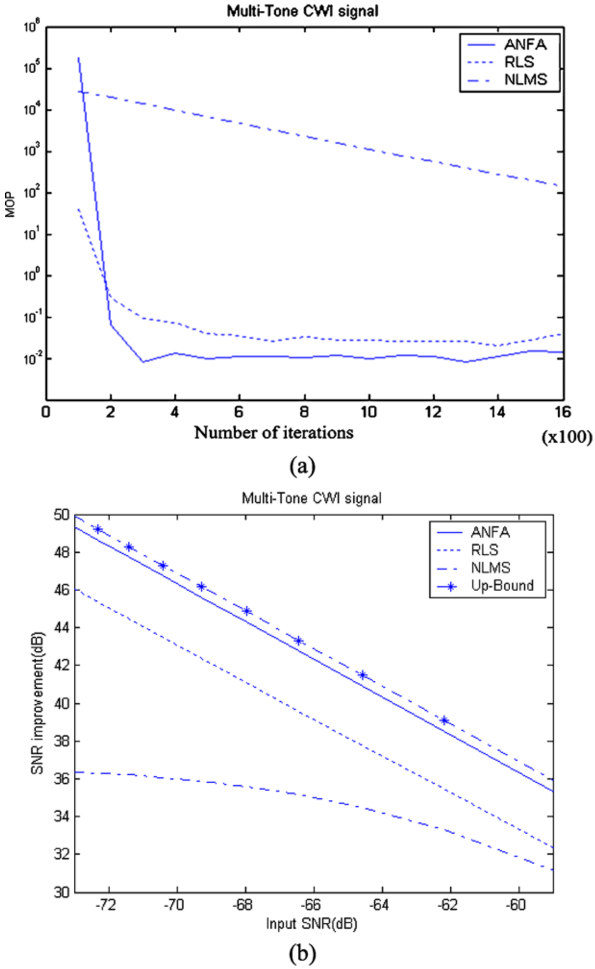

where $Z(n)$represents the baseband GPS spreading signal, $B(n) \oplus CA(n)$. In our simulation, the linear tapped delay predictors with NLMS and RLS adaptive algorithms are compared with the proposed MAGN-based ANFA method. The tap number of the predictors is 10. The step size of the NLMS is set to 0.01. The initial diagonal elements of the error covariance matrix and the forgetting factor of the RLS are set to 0.01 and 1.0, respectively. For the ANFA, the forgetting factor λ_0 is set to 0.8. The pole radius ρ_0 is set to 0.84 in the single- and multi-tone CWI cases, and 0.89 in the pulsed and swept CWI cases. The down-conversion IF is fixed at 1.25 MHz, and sampling rate is chosen as 5 MHz. The variance of the AWGN is held constant at $\sigma^2 = 0.01$. In the MOP simulation, the total jamming-to-signal ratio (JSR) is 73 dB, and the first 1600 samples are adopted. In the steady-state simulation, 9500 samples are computed, and the last 1000 samples are used to compute the SNR improvement.

(A) *Single-tone CWI jamming.* Figure 2 presents the SNR improvements and averaged MOP for single-tone CWI. The frequency of the interference signal is set

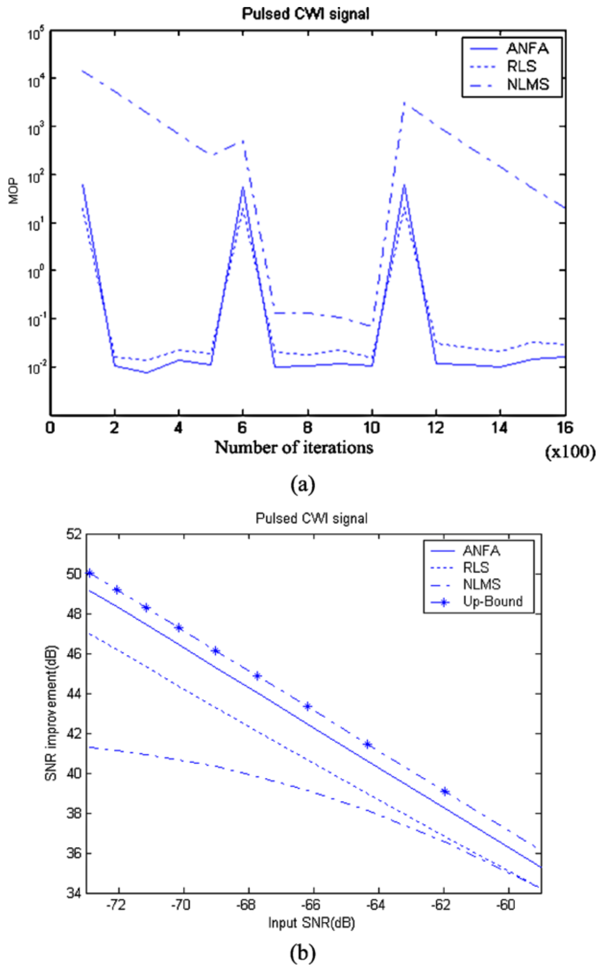

Fig. 4 (**a**) Average MOP $Y_{\mathrm{MOP}}(k)$ vs. the number of iterations and (**b**) SNR improvement for pulsed interference suppression

to 1.2 MHz, and the input SNR is varied from −72 to −60 dB. Figure 2(a) shows that the ANFA scheme is superior in both convergence speed and prediction error. The MOP can decline significantly to 10^{-2} in 200 iterations, while the other methods reach the steady state slowly and have larger MOP. Obviously, the NLMS is the worst one in the convergence comparisons. In the steady-state condition, the SNR improvements of ANFA are also better than both RLS and NLMS schemes. The average SNR improvements are 8.17 and 1.98 dB higher than those of the NLMS and RLS, respectively.

(B) *Multi-tone CWI jamming.* The multi-tone test results are demonstrated in Fig. 3. The offset frequencies are set at 0.5, 1.3, and 1.8 MHz. The ANFA method performs with faster convergence ability and better SNR improvements than both RLS and NLMS. The MOP can be reduced markedly to 0.01 in 300 iterations, whereas the other approaches reach the steady state after 600 iterations and offer the larger

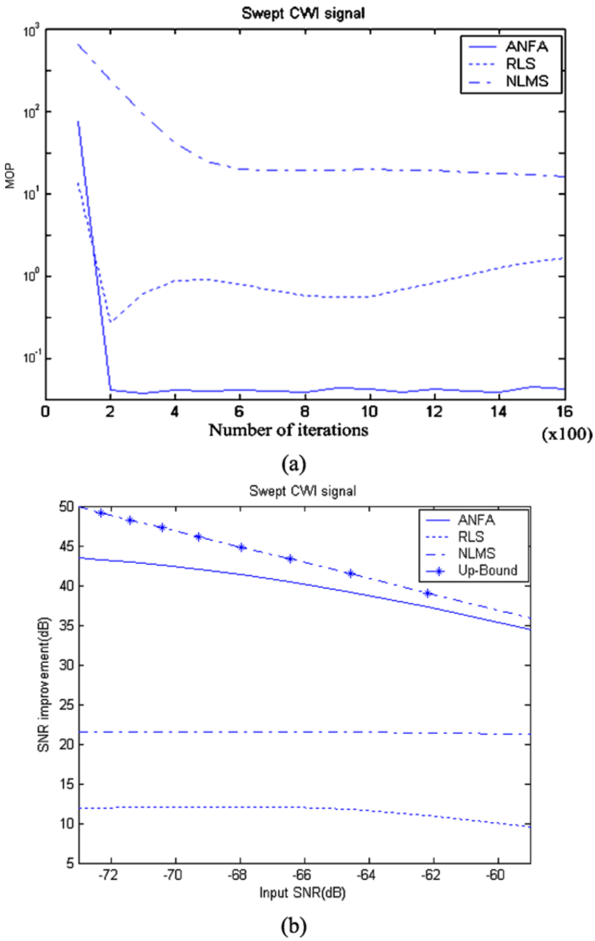

Fig. 5 (**a**) Average MOP $Y_{\mathrm{MOP}}(k)$ vs. the number of iterations and (**b**) SNR improvement for swept interference suppression

MOP. On average, the ANFA scheme can offer 8.94 and 3.20 dB more in terms of SNR improvements than these two methods, respectively.

(C) *Pulsed CWI (FM) jamming.* The frequency offset is chosen as 1.2 MHz. The on-interval is from the 1st to the 500th samples, and the off-interval is from the 501st to the 1000th iteration points. Figure 4(a) indicates that the ANFA method has faster convergence ability compared with the RLS and NLMS methods during both the on- and off-intervals. The ANFA can perform 1.84 and 4.5 dB more in terms of SNR improvements than the RLS and NLMS, respectively.

(D) *Swept CWI jamming.* The simulation results of linear FM are shown in Fig. 5. The sweep rate is set to 526 MHz/s. The starting frequency is set to 0.75 MHz, and the ending frequency is 1.75 MHz. It can be seen that the RLS method performs poorly at estimating non-stationary interference signals. Since the step size of the NLMS filter is constant, the corresponding convergence rate is very slow and limited. The ANFA method accomplishes performances superior to the NLMS and RLS schemes both in

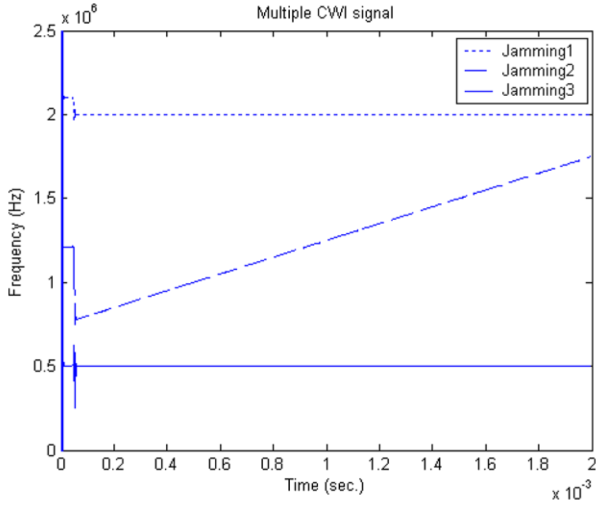

Fig. 6 The frequency estimation of the jamming signal by the ANFA method

transient and steady states. It can offer 19.19 and 29.03 dB more SNR improvement over the NLMS and RLS methods, respectively.

(E) *Frequency parameter estimation.* The simulation results of estimating the instantaneous frequency are presented in Fig. 6. The interfering signals consist of three components. The first is a swept CWI signal sweeping from 0.75 to 1.75 MHz in 2 ms, and the others are fixed CWI signals with frequencies of 0.5 and 2 MHz. It can be seen that the ANFA can track the interference waveform swiftly within 0.05 ms time slot. Moreover, these frequencies and frequency rate parameters can be estimated correctly and successfully by the ANFA method.

6 Conclusions

This paper presents an ANFA structure trained with a MAGN algorithm applied for GPS interference cancellation and frequency parameter estimation. The variable step size, which is optimized with respect to the reduction of MOP, is employed in the MAGN method to speed up the convergence and improve the tracking capability. On average, the proposed scheme yields an SNR improvement that is 10.20 and 9.013 dB better than those of the NLMS and RLS, respectively. The simulation results demonstrate that the ANFA can achieve superior SNR improvement and lower residual interference level than those of the conventional adaptive filter in the interference conditions of interest.

Acknowledgements The authors would like to thank the National Science Council of the Republic of China, Taiwan for financially supporting this research under Contract Nos. NSC 97-2221-E-150-036 and NSC 96-2221-E-150-003-.

References

1. M.G. Amin, L. Shao, A.R. Lindsey, Subspace array processing for the suppression of FM jamming in GPS receiver. IEEE Trans. Aerosp. Electron. Syst. **40**(1), 80–92 (2004)
2. S. Barbarossa, A. Scaglione, Adaptive time-varying cancellation of wideband interference in spread spectrum communications based on time-frequency distributions. IEEE Trans. Signal Process. **47**(4), 957–965 (1999)
3. P.T. Capozza, B.J. Holland, T.M. Hopkinson, R.L. Landrau, A single-chip narrow-band frequency-domain excisor for a global positioning system (GPS) receiver. IEEE J. Solid-State Circuits **35**(3), 401–411 (2002)
4. P.S.R. Diniz, J.E. Cousseau, A. Antoniou, Improved parallel realisation of IIR adaptive filters. IEE Proc., G, Circuits Devices Syst. **140**(5), 322–328 (1993)
5. Y. Liu, T.I. Laakso, P.S.R. Diniz, A complex adaptive notch filter algorithm with optimal convergence factor, in *European Conference on Circuit Theory and Design (ECCTD'01)*, III (2001), pp. 349–352
6. A. Nehorai, A minimal parameter adaptive notch filter with constrained poles and zeros. IEEE Trans. Acoust. Speech Signal Process. **33**(4), 983–996 (1985)
7. S.C. Pei, C.C. Tseng, Complex adaptive IIR notch filter algorithm and its applications. IEEE Trans. Circuits Syst. II, **41**(2), 158–163 (1994)
8. L.A. Rusch, H.V. Poor, Narrowband interference suppression in CDMA spread spectrum communications. IEEE Trans. Commun. **42**, 1969–1979 (1994)
9. L. Wang, H. Zhao, G. Xiong, S. Zhang, AM-FM interference suppression for GPS receivers based on time-frequency analysis and synthesis, in *MAPE IEEE International Symposium Microwave, Antenna, Propagation and EMC Technologies for Wireless Communications, 2005. MAPE 2005. IEEE International Symposium*, 2 (2005) pp. 1378–1381
10. C.-L. Wu, *Adaptive digital all-pass based notch filters*, M.E. Thesis, GICE, Nat. Taiwan Univ., Taipei, Taiwan, 2002